

Regiospecific Oximato Coordination at the Oxygen Site: Ligand Design and Low-Spin Mn^{II} and Fe^{II/III} Species

Sanjib Ganguly, Soma Karmakar, Chandan Kumar Pal, and Animesh Chakravorty*

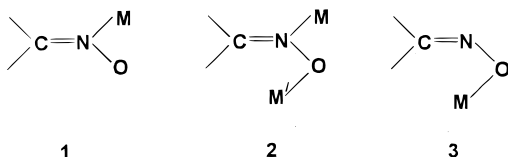
Department of Inorganic Chemistry, Indian Association for the Cultivation of Science, Calcutta 700 032, India

Received June 15, 1999

The (pyridylazo)oxime ligand (C₅H₄N)N=NC(=NOH)C₆H₄R(*p*), HRL (R = H, Me), has been synthesized with the objective of promoting the very rare mononuclear oximato-*O* coordination. The synthesis involves hydrazone nitrosation. HRL reacts with M(ClO₄)₂·6H₂O, affording [M(RL)₂] (M = Mn, Fe), and X-ray structure determinations have indeed revealed the presence of the desired oximato-*O* coordination mode in the distorted octahedral MN₄O₂ sphere characterized by a 2-fold axis of symmetry relating the two tridentate ligands, all chelate rings being five-membered. The M–N and M–O distances are relatively short (1.84–1.99 Å), consistent with spin-pairing (M = Mn, *S* = 1/2; M = Fe, *S* = 0). The M–N bond length trend, Mn^{II} > Fe^{II}, is in accord with the larger radius of the low-spin Mn^{II} atom. The M–O length order is, however, Mn^{II} < Fe^{II}. This reversal occurs because of the rigidity of the ligand skeleton. Significant M–azo back-bonding is present (N=N length ~1.30 Å). [Mn(RL)₂] displays hyperfine-split axial EPR spectra (*g*_{||} ~ 1.98, *g*_⊥ ~ 2.06, *A*_{||} ~ 170 G, *A*_⊥ ~ 65 G) in frozen solution as well as in polycrystalline [Fe(RL)₂] lattices. The quasireversible Fe(III)/Fe(II) couple of [Fe(RL)₂] has *E*_{1/2} ~ 0.7 V. The oxidized complex [Fe(RL)₂]PF₆ has been electrosynthesized. It is low-spin (*S* = 1/2) and displays axial EPR spectra (*g*_{||} ~ 1.98, *g*_⊥ ~ 2.14) in frozen solution. The Mn(II) → Mn(III) oxidation (~1.0 V) in [Mn(RL)₂] is irreversible. Crystal data for [Mn(HL)₂]·CH₂Cl₂: crystal system monoclinic, space group *I*2/a, *a* = 14.142(7) Å, *b* = 10.721(7) Å, *c* = 16.933(10) Å, β = 93.01(4)°, *Z* = 4. Crystal data for [Fe(HL)₂]·CH₂Cl₂: crystal system monoclinic, space group *I*2/a, *a* = 14.254(6) Å, *b* = 10.742(6) Å, *c* = 16.719(8) Å, β = 92.35(4)°, *Z* = 4.

Introduction

Oximes, like Schiff bases, have persistently played a notable role in the development of transition metal coordination chemistry,¹ and unabated activity is current in this area.^{2–6} In mononuclear systems, oximes bind metal ions virtually universally via the N site only, as in **1**. In contrast, the best known

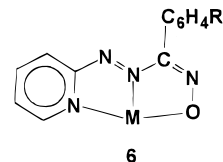


examples of O-binding occur in multinuclear assemblies incorporating the two-atom bridging mode **2** wherein the N site is also engaged.^{7–9} Regiospecific mononuclear binding at the O site as in **3** remains a matter of curiosity.¹⁰

The present work was undertaken with the objective of realizing the coordination mode **3** in a rational manner. For this purpose, a suitable ligand system was designed. It afforded manganese(II) and iron(II,III) chelates wherein the presence of O-binding was authenticated by structure determinations. A notable magnetic feature is the efficacy of **3** in sustaining low-spin character even in the case of bivalent manganese.

Results and Discussion

Syntheses. Ligands and Complexes. The concerned ligand system HRL (H refers to the dissociable oxime hydrogen) is a (pyridylazo)oxime synthesized from 2-hydrazinopyridine as in shown Scheme 1, which also outlines the synthesis of [Mn^{II}(RL)₂], [Fe^{II}(RL)₂], and [Fe^{III}(RL)₂]PF₆. The binding mode (vide infra) of RL[−] in these chelates is depicted in **6**.

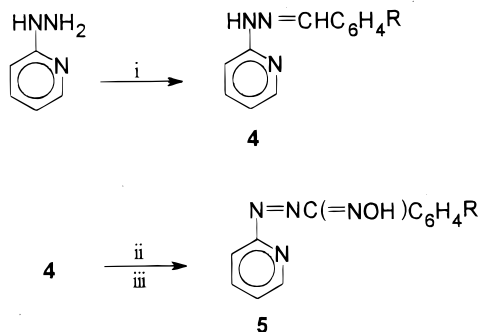


- (1) Chakravorty, A. *Coord. Chem. Rev.* **1974**, *13*, 1.
- (2) (a) Pramanik, K.; Karmakar, S.; Choudhury, S. B.; Chakravorty, A. *Inorg. Chem.* **1997**, *36*, 3562. (b) Karmakar, S.; Choudhury, S. B.; Ganguly, S.; Chakravorty, A. *J. Chem. Soc., Dalton Trans.* **1997**, 585.
- (3) (a) Pavlishchuk, V. V.; Kolotilov, S. V.; Addison, A. W.; Prushan, M. J.; Butcher, R. J.; Thompson, L. K. *Inorg. Chem.* **1999**, *38*, 1759. (b) Martin, J. D.; Abbound, K. A.; Dahmen, K.-H. *Inorg. Chem.* **1998**, *37*, 5811. (c) Fritosky, I. O. *J. Chem. Soc., Dalton Trans.* **1999**, 825.
- (4) (a) Rybak-Akimova, E. V.; Busch, D. H.; Kahol, P. K.; Pinto, N.; Alcock, N. W.; Clase, H. J. *Inorg. Chem.* **1997**, *36*, 510. (b) Cini, R.; Moore, S. J.; Marzilli, L. G. *Inorg. Chem.* **1998**, *37*, 6890. (c) Vernik, I.; Stynes, D. V. *Inorg. Chem.* **1998**, *37*, 10.
- (5) (a) Kukushkin, V. Y.; Belsky, V. K.; Tudela, D. *Inorg. Chem.* **1996**, *35*, 510. (b) Kukushkin, V. Y.; Nishioka, T.; Tudela, D.; Isobe, K.; Kinoshita, I. *Inorg. Chem.* **1997**, *36*, 6157.
- (6) (a) Pal, C. K.; Chattopadhyay, S.; Sinha, C.; Chakravorty, A. *Inorg. Chem.* **1994**, *33*, 6140. (b) Pal, C. K.; Chattopadhyay, S.; Sinha, C.; Chakravorty, A. *Inorg. Chem.* **1996**, *35*, 2442. (c) Manivannan, V.; Dirghangi, B. K.; Pal, C. K.; Chakravorty, A. *Inorg. Chem.* **1997**, *36*, 1526. (d) Ganguly, S.; Manivannan, V.; Chakravorty, A. *J. Chem. Soc., Dalton Trans.* **1998**, 461.

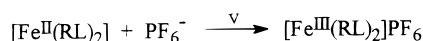
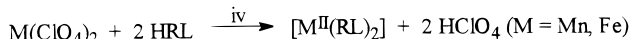
- (7) (a) Manivannan, V.; Datta, S.; Basu, P.; Chakravorty, A. *Inorg. Chem.* **1993**, *32*, 4807 and references therein. (b) Basu, P.; Pal, S.; Chakravorty, A. *Inorg. Chem.* **1988**, *27*, 1848. (c) Pal, S.; Chakravorty, A. *Inorg. Chem.* **1987**, *26*, 4331.
- (8) (a) Birkelbach, F.; Weyhermuller, T.; Lengen, M.; Gerdan, M.; Trautwein, A. X.; Wieghardt, K.; Chaudhuri, P. *J. Chem. Soc., Dalton Trans.* **1997**, 4529. (b) Birkelbach, F.; Florke, U.; Haupt, H.-J.; Butzloff, C.; Trautwein, A. X.; Wieghardt, K.; Chaudhuri, P. *Inorg. Chem.* **1998**, *37*, 2000.
- (9) (a) Dreos, R.; Tazher, G.; Trendafilova, D. H.; Nardin, G.; Randaccio, L. *Inorg. Chem.* **1996**, *35*, 2715. (b) Wu, Z.; Zhou, X.; Zhang, W.; Xu, Z.; You, X.; Huang, X. *J. Chem. Soc., Chem. Commun.* **1994**, 813. (c) Yildiz, S. Z.; Misir, M. N.; Tüfekci, N.; Gok, Y. *Acta Chem. Scand.* **1998**, *52*, 694.

Scheme 1

A. Ligand



B. Complexes



- i. $\text{RC}_6\text{H}_4\text{CHO}$, ethanol-water mixture, stir, 25°C .
- ii. $n\text{-C}_4\text{H}_9\text{NO}_2$, NaOMe, MeOH, boil.
- iii. Dilute NaOH, 25°C , extract with Et_2O , neutralize the aqueous part with 1N H_2SO_4 , 0°C .
- iv. MeOH, stir, 25°C .
- v. MeCN, NH_4PF_6 / TEAP, 0.90 V vs SCE, stir, 25°C .

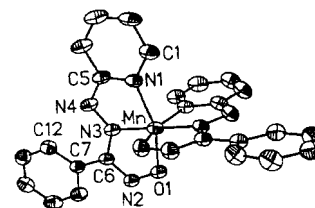
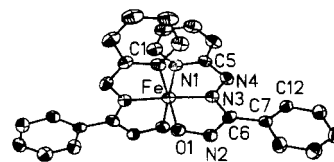
Table 1. Electrochemical^a Data in Acetonitrile Solution at 298 K

compd	$\text{M}^{\text{III}}/\text{M}^{\text{II}}$ $E_{1/2},^b$ V ($\Delta E_p,^c$ mV); $n^{d,e}$	$[-\text{N}=\text{N}-]/[-\text{N}^{\text{---}}\text{N}^-]$ $E_{1/2},^b$ V ($\Delta E_p,^c$ mV)
$[\text{Mn}(\text{HL})_2]$	1.00 ^f	-0.58 (70)
$[\text{Mn}(\text{MeL})_2]$	0.98 ^f	-0.62 (60)
$[\text{Fe}(\text{HL})_2]$	0.70 (90); 1.02	-0.72 (100)
$[\text{Fe}(\text{MeL})_2]$	0.68 (80); 0.98	-0.76 (100)
$[\text{Fe}(\text{HL})_2]\text{PF}_6$	0.70 (90); 1.01	-0.71 (90)
$[\text{Fe}(\text{MeL})_2]\text{PF}_6$	0.68 (90); 0.99	-0.74 (90)

^a At a platinum disk electrode; supporting electrolyte tetraethylammonium perchlorate (TEAP, 0.1 M); scan rate 50 mV s^{-1} ; reference electrode SCE; solute concentration $\sim 10^{-3} \text{ M}$. ^b $E_{1/2}$ is calculated as the average of anodic (E_{pa}) and cathodic (E_{pc}) peak potentials. ^c $\Delta E_p = E_{pa} - E_{pc}$. ^d $n = Q/Q'$, where Q is the observed coulomb count and Q' is the calculated electron count for one-electron transfer. ^e Constant-potential electrolysis was performed at 200 mV below E_{pc} for reduction and at 200 mV above E_{pa} for oxidation. ^f E_{pa} values.

The complexes are uniformly low spin in nature (vide infra) and display characteristic allowed transitions in the 400–750 nm region (see Experimental Section). They are electroactive and display two one-electron responses. Reduction potential data are listed in Table 1. In $[\text{Fe}(\text{RL})_2]$, the Fe(III)/Fe(II) couple near 0.7 V forms the basis for the electrosynthesis of $[\text{Fe}^{\text{III}}(\text{RL})_2]^+$. The voltammograms of $[\text{Fe}(\text{RL})_2]$ (initial scan anodic) and $[\text{Fe}(\text{RL})_2]^+$ (initial scan cathodic) are virtually superposable, suggesting gross structural similarities. The couple near -0.7 V for the complexes is assigned to azo reduction, $[-\text{N}=\text{N}-]/[-\text{N}^{\text{---}}\text{N}^-]$.¹¹ In $[\text{Mn}(\text{RL})_2]$, metal oxidation occurs irreversibly at ~ 1.0 V.

A note on the choice of HRL for achieving binding mode 3 is in order. Azooxime and azopyridine ligands always bind metal

Figure 1. Perspective view and atom-labeling scheme for $[\text{Mn}(\text{HL})_2]$ with all the atoms being represented by 30% probability ellipsoids.Figure 2. Perspective view and atom-labeling scheme for $[\text{Fe}(\text{HL})_2]$ with all the atoms being represented by 30% probability ellipsoids.

ions in the form of five-membered (N^a, N^o) $\text{M}^{2,6-8}$ and (N^a, N^p)- M^{12} chelate rings ($\text{N}^a = \text{azo N}$; $\text{N}^o = \text{oximato N}$; $\text{N}^p = \text{pyridine N}$). In HRL, the azooxime and azopyridine functions have been juxtaposed. If coordination via N sites alone was to take place in the tridentate bicyclic chelation of RL^- , only one chelate ring would be five-membered, the other being four-membered and presumably unstable. This difficulty is circumvented via a one-atom shift of the oximato coordination from the N^o to the O^o site, and both chelate rings become five-membered.

Structures. Both $[\text{Mn}(\text{HL})_2] \cdot \text{CH}_2\text{Cl}_2$ and $[\text{Fe}(\text{HL})_2] \cdot \text{CH}_2\text{Cl}_2$ afforded single crystals, thus providing a rare opportunity for observing the subtle differences between bond parameters of low-spin Mn^{II} and Fe^{II} held in the same coordination environment. As expected, the two structures are isomorphous and nearly isometric. Molecular views and atom-numbering schemes are shown in Figures 1 and 2. Selected bond parameters are listed in Table 2. The metal atom, as well as the dichloromethane carbon atom, lies on a crystallographic 2-fold axis. The two ligands are thus equivalent by symmetry. The HL^- ligand binds in a meridional tridentate fashion via O^o , N^a , and N^p atoms, forming the distorted octahedral MN_4O_2 coordination sphere as in 6.

This work provides the first quantitation of $\text{Mn}-\text{N}^p$, 1.990(3) Å, and $\text{Mn}-\text{O}^o$, 1.891(3) Å, lengths in a low-spin manganese(II) complex. The $\text{Mn}-\text{N}^a$ length, 1.873(3) Å, is significantly shorter than the average values (1.92–1.96 Å) observed in two structurally characterized low-spin azooxime complexes incorporating (N^a, N^o)Mn chelation.¹³ There is a large radial contraction¹⁴ due to spin-pairing (range of $\text{Mn}^{\text{II}}-\text{N}$ and $\text{Mn}^{\text{II}}-\text{O}$ distances in high-spin species is 2.1–2.3 Å).

(10) A few oximato-*O*-bridged dimers are known, and a nitrosolate with *O*-binding has been described: (a) Ruiz, R.; Sanz, J.; Lloret, F.; Julve, M.; Fans, J.; Bois, C.; Munoz, M. C. *J. Chem. Soc., Dalton Trans.* **1993**, 3035. (b) Colacio, E.; Dominguez-Vera, J. M.; Escuer, A.; Kivekas, R.; Romerosa, A. *Inorg. Chem.* **1994**, *33*, 3914. (c) Gouzerh, P.; Jeanin, Y.; Rocchiccioli-Deltcheff, C.; Valentini, F. *J. Coord. Chem.* **1979**, *9*, 221.

(11) (a) Shivakumar, M.; Pramanik, K.; Ghosh, P.; Chakravorty, A. *Inorg. Chem.* **1998**, *37*, 5968. (b) Ackermann, M. N.; Barton, C. R.; Deodene, C. J.; Specht, E. M.; Keill, S. C.; Schreiber, W. E.; Kim, H. *Inorg. Chem.* **1989**, *28*, 397. (c) Kaim, W.; Kohlmann, S. *Inorg. Chem.* **1987**, *26*, 68.
 (12) (a) Shivakumar, M.; Pramanik, K.; Ghosh, P.; Chakravorty, A. *J. Chem. Soc., Chem. Commun.* **1998**, 2103. (b) Goswami, S.; Chakravarty, A. R.; Chakravorty, A. *Inorg. Chem.* **1981**, *20*, 2246. (c) Seal, A.; Roy, S. *Acta Crystallogr.* **1984**, *40C*, 929. (d) Ghosh, B. K.; Mukhopadhyay, A.; Goswami, S.; Chakravorty, A. *Inorg. Chem.* **1984**, *23*, 4633. (e) Krause, R. A.; Krause, K. *Inorg. Chem.* **1980**, *19*, 2600. (f) Majumdar, P.; Peng, S.-M.; Goswami, S. *J. Chem. Soc., Dalton Trans.* **1998**, 1569. (g) Kharmowphlang, W.; Choudhury, S.; Deb, A. K.; Goswami, S. *Inorg. Chem.* **1995**, *35*, 3826.
 (13) (a) Karmakar, S.; Choudhury, S. B.; Chakravorty, A. *Inorg. Chem.* **1994**, *33*, 6148 and references therein. (b) Chattopadhyay, S.; Basu, P.; Pal, S.; Chakravorty, A. *J. Chem. Soc., Dalton Trans.* **1990**, 3829.
 (14) (a) Shannon, R. D. *Acta Crystallogr.* **1976**, *A32*, 751. (b) Shannon, R. D.; Prewitt, C. T. *Acta Crystallogr.* **1969**, *B25*, 925.

Table 2. Selected Bond Distances (Å) and Angles (deg) and Their Estimated Standard Deviations for $[M(HL)_2] \cdot CH_2Cl_2$

	M = Mn	M = Fe
Distances		
M–N1	1.990(3)	1.968(6)
M–N3	1.873(3)	1.841(7)
M–O1	1.891(3)	1.912(5)
N2–O1	1.357(4)	1.333(8)
N3–N4	1.322(4)	1.298(8)
Angles		
N3–M–N3A	179.5(2)	177.4(4)
N3–M–O1	80.3(1)	81.2(3)
N3–M–O1A	100.1(1)	96.9(3)
N3–M–N1A	101.9(1)	103.0(3)
N3–M–N1	77.7(1)	78.9(3)
O1–M–O1A	93.6(2)	92.7(4)
O1–M–N1	157.9(1)	160.0(3)
N1–M–N1A	89.7(2)	89.9(4)
O1A–M–N1	92.6(1)	92.1(2)

Table 3. Magnetic Moment and EPR Spectral Data (X-band)

compd	magnetic moment ^a μ_{eff}, μ_B	EPR				
		g_{\parallel}	g_{\perp}	A_{\parallel}, G	A_{\perp}, G	
$[Mn(HL)_2]^b$	1.93	<i>c</i>	1.982	2.065	170	60
		<i>d</i>	1.980	2.063	160	65
$[Mn(MeL)_2]^c$	1.89	<i>c</i>	1.977	2.062	170	60
		<i>d</i>	1.978	2.060	170	65
$[Fe(HL)_2]PF_6$	1.98	<i>c</i>	1.987	2.137		
$[Fe(MeL)_2]PF_6$	2.01	<i>c</i>	1.982	2.141		

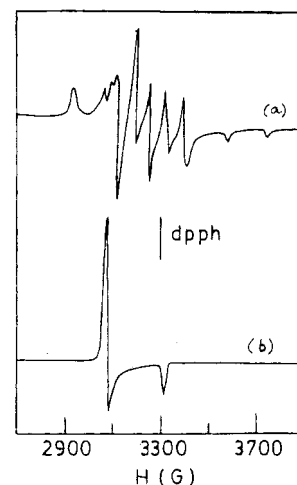
^a In solid state (298 K). ^b In dichloromethane–toluene solution (298 K), $g_{\text{iso}} = 2.035$, $A_{\text{iso}} = 94$ G. ^c In 1:1 dichloromethane–toluene solution at 77 K. ^d In polycrystalline $[Fe(RL)_2]$ host with 1% $[Mn(RL)_2]$ as dopant. ^e In dichloromethane–toluene solution (298 K), $g_{\text{iso}} = 2.041$, $A_{\text{iso}} = 90$ G.

The Fe–N^a, 1.841(7) Å, and Fe–N^p, 1.968(6) Å, distances are ~ 0.03 Å shorter than Mn–N^a and Mn–N^p distances. In effect, the iron(II) atom is drawn closer to the azopyridine fragment and this is also reflected in the larger N^a–M–N^p bite angle for iron (M = Fe, 78.9(3)°; M = Mn, 77.7(1)°). These observations are consistent with the trend in low-spin radii:¹⁴ $Mn^{II} > Fe^{II}$. However, the Fe–O^o distance, 1.912(5) Å, is slightly longer than the Mn–O^o distance. The reason for this is the inflexibility of the conjugated ligand frame, the frames of the two complexes being nearly exactly superposable. As the smaller iron(II) atom adjusts to N^p, N^a chelation, it becomes distanced from O^o.

There is a significant $t_2 \rightarrow \pi^*$ (azo) back-bonding component^{11a} to the strong N^p, N^a affinity for the bivalent d^5 and d^6 ions as seen in the relatively long, ~ 1.30 Å, azo N=N length (~ 1.25 Å in uncoordinated state).¹⁵ The ready accessibility of the π^* -(azo) orbital for back-bonding is consistent with its relatively low energy as reflected in the reduction potential data; vide supra.

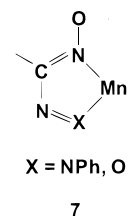
Spin States and EPR Spectra. The $[Fe(RL)_2]$ complexes are diamagnetic while $[Mn(RL)_2]$ and $[Fe(RL)_2]^+$ have a low-spin d^5 configuration ($S = 1/2$). Magnetic moments and EPR spectral data are listed in Table 3. In dichloromethane–toluene solution at room temperature, $[Mn(RL)_2]$ displays a six-line (^{55}Mn , $I = 5/2$) isotropic EPR spectrum with $A_{\text{iso}} \sim 90$ G. When the solution is frozen at 77 K, the spectrum becomes axial, both components being hyperfine-split. A virtually identical spectrum is furnished by polycrystalline $[Fe(RL)_2]$ doped with 1% $[Mn(RL)_2]$ (Figure 3, Table 3).

In principle, $[Mn(RL)_2]$ has rhombic symmetry, but in practice, the rhombic component of the ligand field is not

**Figure 3.** (a) X-band EPR spectrum of polycrystalline $[Fe(HL)_2]$ doped with 1% $[Mn(HL)_2]$ at 298 K. (b) X-band EPR spectrum of $[Fe(HL)_2]PF_6$ in frozen 1:1 dichloromethane–toluene solution at 77 K.

resolved. The EPR spectrum of $[Fe(RL)_2]PF_6$ in frozen glass is also axial,¹⁶ Figure 3.

Among bivalent 3d ions, manganese(II) has the highest spin-pairing energy,¹⁷ and only very strong-field ligands can induce low-spin character. Such species are therefore relatively uncommon.^{13a} It has been argued that chelate rings of type $7^{10c,13a,18}$ incorporating oximato-*N* binding can induce low-spin



character in manganese(II), consistent with the large ligand field splitting associated with such binding.¹⁹ A notable finding of the present work is that oximato-*O* coordination can also be strong enough (note the short M–O distances) and as effective in sustaining spin-pairing.

Concluding Remarks

It is demonstrated that the rare mononuclear oximato-*O* coordination is achievable via juxtaposition of azopyridine and azooxime functions. In spite of O-binding, bischelation of RL^- is able to induce a low-spin configuration for manganese(II) in an axial ligand field. The rigidity of the ligand skeleton finds expression in the bond length trends: M–N, $Mn^{II} > Fe^{II}$ but M–O, $Mn^{II} < Fe^{II}$.

Facile one-electron azo reduction characterizes coordinated RL^- . The reduced ligand can be stabilized via binding to Co^{III} . With 4d and 5d elements, HRL affords mono- and multinuclear species with variable azo reduction levels. These and other findings are under scrutiny and will be reported in the future.

(15) (a) Mostad, A.; Romming, C. *Acta Chem. Scand.* **1971**, *25*, 3561. (b) Chang, C. H.; Porter, R. F.; Brauer, S. H. *J. Am. Chem. Soc.* **1970**, *92*, 5313. (c) Roy, T.; Sengupta, S. P. *Cryst. Struct. Commun.* **1980**, *9*, 965.

(16) A low-spin $Fe^{III}N_4O_2$ system affording a rhombic spectrum is known: Karmakar, S.; Chakravorty, A. *Inorg. Chem.* **1996**, *35*, 1935.

(17) Lever, A. B. P. *Inorganic Electronic Spectroscopy*, 2nd ed.; Elsevier: New York, 1984; p 751.

(18) (a) Basu, P.; Chakravorty, A. *Inorg. Chem.* **1992**, *31*, 4980. (b) Basu, P.; Chakravorty, A. *J. Chem. Soc., Chem. Commun.* **1992**, 809.

(19) Mohanty, J. G.; Singh, R. P.; Chakravorty, A. *Inorg. Chem.* **1975**, *14*, 2178.

Experimental Section

Physical Measurements. A Hitachi 330 spectrophotometer was used to record UV-vis spectra. EPR spectra were recorded in the X-band on a Varian E-109 spectrometer fitted with a quartz dewar. The spectra were calibrated with respect to DPPH ($g = 2.0037$). Magnetic susceptibilities were measured with a model 155 PAR vibrating-sample magnetometer fitted with a Walker Scientific L75FBAL magnet. A Perkin-Elmer 2400 Series(II) elemental analyzer was used to collect microanalytical data (CHN). Electrochemical measurements were performed under a nitrogen atmosphere on a PAR 370-4 electrochemistry system using solvents and supporting electrolytes purified/prepared as before.²⁰ All potentials are referenced to the saturated calomel electrode (SCE). Solution electrical conductivities were measured with the help of a Philips PR 9500 bridge, the solute concentrations being $\sim 10^{-3}$ M.

Synthesis of Ligands, HRL, 5. The details of the synthesis are given below for the R = H ligand (the R = Me ligand was prepared similarly).

2-(Pyridylazo)benzaloxime, HHL, 5 (R = H). To a 1:1 ethanolic solution (yellow) of 2.50 g (0.023 mol) of 2-hydrazinopyridine was added dropwise 2.43 g (0.022 mol) of benzaldehyde. The contents were allowed to stir for 2 h, and a white precipitate of the hydrazone, **4** (R = H), separated out. This was collected, washed with 1:1 aqueous ethanol, and then dried in vacuo over fused CaCl₂. Yield: 3.60 g (80%).

To a suspension of 3.60 g (0.018 mol) the hydrazone **4** in 25 mL of dry ethanol was added 1.85 g (0.018 mol) of freshly prepared *n*-BuNO₂. To this mixture was added a solution of sodium methoxide (prepared by refluxing 0.85 g of metallic sodium in 25 mL of dry methanol). The mass was heated to reflux for 2 h, affording an intensely red solution, which was cooled and filtered into an ice-cold solution of sodium hydroxide (prepared by dissolving 1.0 g of NaOH in 100 mL of water). After 12 h, the solution was extracted with diethyl ether. The aqueous layer was separated from the mixture, cooled to 0 °C, and finally acidified with a 1 N ice-cold solution of sulfuric acid to neutral pH when the HHL ligand separated out as a yellow precipitate. This was filtered off, washed with water, and dried in vacuo over fused CaCl₂. Yield: 1.80 g (44%). Anal. Calcd for **5** (R = H), C₁₂H₁₀N₄O: C, 63.72; H, 4.42; N, 24.77. Found: C, 63.65; H, 4.38; N, 24.68. Mp: 103–105 °C.

Anal. Calcd for **5** (R = Me), C₁₃H₁₂N₄O: C, 65.00; H, 5.00; N, 23.33. Found: C, 64.91; H, 5.05; N, 23.26. Mp: 100–102 °C.

Synthesis of Complexes. Dichloromethane Adduct of Bis[(2-pyridylazo)-1-benzaldoximate]manganese(II), [Mn(HL)₂]·CH₂Cl₂. The complex was prepared by adding a methanolic solution (10 mL) of HHL (0.066 g, 0.29 mmol) to a solution containing Mn(ClO₄)₂·6H₂O (0.050 g, 0.14 mmol), and the deep violet solution so formed was stirred for 2 h. The deposited dark violet crystalline solid was filtered off, washed several times with 1:1 aqueous methanol, and dried in vacuo over fused CaCl₂. It was finally recrystallized from dichloromethane–hexane. Yield: 0.062 g (84%). Anal. Calcd for C₂₅H₂₀N₈O₂·Cl₂Mn: C, 50.85; H, 3.59; N, 18.98. Found: C, 50.78; H, 3.56; N, 18.90. UV-vis (CH₂Cl₂; λ_{max}, nm (ε, M⁻¹ cm⁻¹)): 650 (4200); 550 (5200); 490 (4400); 420 (5200).

The complex [Mn(MeL)₂]·CH₂Cl₂ was prepared similarly. Anal. Calcd for C₂₇H₂₂N₈O₂Cl₂Mn: C, 52.68; H, 3.57; N, 18.21. Found: C, 52.59; H, 3.54; N, 18.27. UV-vis (CH₂Cl₂; λ_{max}, nm (ε, M⁻¹ cm⁻¹)): 640 (4400); 550 (5500); 480 (4800); 410 (5300).

Dichloromethane Adduct of Bis[(2-pyridylazo)-1-benzaldoximate]iron(II), [Fe(HL)₂]·CH₂Cl₂. The dark green complex was prepared by the same procedure as above, replacing Mn(ClO₄)₂·6H₂O by Fe(ClO₄)₂·6H₂O. Yield: 0.062 g (90%). Anal. Calcd for C₂₅H₂₀N₈O₂Cl₂·Fe: C, 50.77; H, 3.38; N, 18.96. Found: C, 50.69; H, 3.33; N, 18.88. UV-vis (CH₂Cl₂; λ_{max}, nm (ε, M⁻¹ cm⁻¹)): 700 (6600); 540 (5000); 475 (5600); 400 (10 600).

Anal. Calcd for [Fe(MeL)₂]·CH₂Cl₂, C₂₇H₂₄N₈O₂Cl₂·Fe: C, 52.36; H, 3.88; N, 18.10. Found: C, 52.29; H, 3.83; N, 18.15. UV-vis (CH₂Cl₂; λ_{max}, nm (ε, M⁻¹ cm⁻¹)): 700 (6300); 550 (4900); 475 (5200); 400 (10 100).

Table 4. Crystallographic Data for [M(HL)₂]·CH₂Cl₂

	M = Mn	M = Fe
empirical formula	C ₂₅ H ₁₉ N ₈ O ₂ Cl ₂ Mn	C ₂₅ H ₁₉ N ₈ O ₂ Cl ₂ Fe
fw	589.32	590.23
space group	<i>I</i> 2/a	<i>I</i> 2/a
<i>a</i> , Å	14.142(7)	14.254(6)
<i>b</i> , Å	10.721(7)	10.742(6)
<i>c</i> , Å	16.933(10)	16.719(8)
β, deg	93.01(4)	92.35(4)
<i>V</i> , Å ³	2570(3)	2558(2)
<i>Z</i>	4	4
<i>T</i> , °C	293(2)	293(2)
λ, Å	0.710 73	0.710 73
ρ _{calcd} , g cm ⁻³	1.523	1.533
μ, cm ⁻¹	7.62	8.39
R1 ^a [<i>I</i> > 2σ(<i>I</i>)]	0.0547	0.0821
wR2 ^b [<i>I</i> > 2σ(<i>I</i>)]	0.1251	0.1633
GO ^c	1.045	1.042

$$^a R1 = \sum ||F_o| - |F_c|| / \sum |F_o|. \quad ^b wR2 = [\sum w(F_o^2 - F_c^2)^2 / \sum w(F_o^2)]^{1/2}.$$

Bis[(2-pyridylazo)-1-benzaldoximate]iron(III) Hexafluorophosphate, [Fe(HL)₂]PF₆. [Fe(HL)₂] (0.05 g, 0.1 mmol) was dissolved in 25 mL of acetonitrile, and NH₄PF₆ (0.016 g, 0.1 mmol) was added as the supporting electrolyte. The dark green mixture was stirred at room temperature for 0.25 h and then subjected to exhaustive oxidation at 0.9 V vs SCE under nitrogen. The oxidation was stopped when the coulomb count corresponded to one-electron oxidation and the color of the solution became reddish pink. The solvent was evaporated in vacuo to obtain the brown solid in pure form. Yield: 0.059 g (92%). Anal. Calcd for C₂₄H₁₈N₈O₂PF₆·Fe: C, 42.17; H, 2.64; N, 16.39. Found: C, 42.13; H, 2.63; N, 16.31. UV-vis (CH₂Cl₂; λ_{max}, nm (ε, M⁻¹ cm⁻¹)): 560 (1700); 440 (1800).

The complex [Fe(MeL)₂]PF₆ was electrosynthesized in a similar fashion. Anal. Calcd for C₂₆H₂₂N₈O₂PF₆·Fe: C, 45.95; H, 3.24; N, 16.49. Found: C, 45.88; H, 3.21; N, 16.41. UV-vis (CH₂Cl₂; λ_{max}, nm (ε, M⁻¹ cm⁻¹)): 565 (1800); 445 (1900).

X-ray Structure Determinations. Crystals of [Mn(HL)₂]·CH₂Cl₂ (0.3 × 0.4 × 0.3 mm) and [Fe(HL)₂]·CH₂Cl₂ (0.4 × 0.3 × 0.3 mm) were grown by slow diffusion of hexane into dichloromethane solutions. For both complexes, cell parameters were determined by the least-squares fit of 30 machine-centered reflections (2θ 15–30°). Data were collected by the ω-scan technique in the 2θ range 3–50° on a Siemens R3m/V four-circle diffractometer with graphite-monochromated Mo Kα radiation (λ = 0.710 73 Å). Two check reflections measured after every 98 reflections showed no intensity reduction. Data were corrected for Lorentz–polarization effects, and an empirical absorption correction was performed on both sets of data on the basis of azimuthal scans²¹ of six reflections. For [Mn(HL)₂]·CH₂Cl₂, 2453 reflections were collected, of which 2280 were unique and 1673 satisfying *I* > 2σ(*I*) were used for structure solution. In the case of [Fe(HL)₂]·CH₂Cl₂, the corresponding numbers are 2442, 2257, and 1023, respectively.

All calculations for data reduction and structure solution and refinement were done using programs of SHELXTL, Version 5.03.²² Both the structures were solved by direct methods and were refined by full-matrix least-squares calculations on *F*². All non-hydrogen atoms were refined anisotropically, while hydrogen atoms were included in calculated positions. Significant crystal data are listed in Table 4.

Acknowledgment. Financial support from the Indian National Science Academy, the Department of Science and Technology, and the Council of Scientific and Industrial Research, New Delhi, is gratefully acknowledged. Affiliation with the Jawaharlal Nehru Centre for Advanced Scientific Research, Bangalore, is also acknowledged.

Supporting Information Available: X-ray crystallographic files, in CIF format, for [Mn(HL)₂]·CH₂Cl₂ and [Fe(HL)₂]·CH₂Cl₂. The material is available free of charge via the Internet at <http://pubs.acs.org>.

IC9907011

(20) (a) Basu, P.; Choudhury, S. B.; Pal, S.; Chakravorty, A. *Inorg. Chem.* **1989**, *28*, 2680. (b) Lahiri, G. K.; Bhattacharya, S.; Ghosh, B. K.; Chakravorty, A. *Inorg. Chem.* **1987**, *26*, 4324.

(21) North, A. C. T.; Phillips, D. C.; Mathews, F. S. *Acta Crystallogr.* **1968**, *A24*, 351.
(22) Sheldrick, G. M. *SHELXTL*, Version 5.03; Siemens Analytical Instruments Inc.: Madison, WI, 1994.